Matthew Lambrechts (22232000)
Nora De Vleeschouwer (48602100)

20 December 2024

LGBIO2072 - Project 2
Data Analysis

# 1 Neural Data

We have access to the measurements of 5 quantities for 6 trials of 8 reaching movements towards 8 different targets. The 5 quantities are: shoulder angle, elbow angle, hand's $x$ and $y$ coordinates and spike (binary variable). The data sampled at 200 [Hz] are recorded over a timespan of 4 [s] on average but the reaching movements last 1 [s] on average because they are short, 6 [cm] on average. Hence, we should do some preprocessing for each measurement to only keep its portion where the reaching movement occurs. For each reaching movement, each trial is measured over a slightly different timespan so we cannot just choose a subinterval of time common to all the trials because for one trial the reaching movement might occur during that subinterval of time but for another trial it might not be the case. Instead, for each reaching movement, after we took a look at the measurements, we choose a threshold for one of the 5 quantities, given in Table 1, reached during the reaching movement and for each trial, the corresponding time is the center of the subinterval of 1 [s] of interest as we know that the reaching movements last on average 1 [s]. Thus for each reaching movement, we obtain the measurements of the 5 quantities over a timespan of 1 [s] for each trial.

| quantity | handxpos | handxpos | shoang | shoang | elbang | elbang | elbang | shoang |
|---|---|---|---|---|---|---|---|---|
| threshold | 25 | 20 | 0.9 | 1 | 1.7 | 1.9 | 1.7 | 0.7 |

Table 1: Thresholds for Targets 1 to 8 from left to right for Preprocessing

Finally, for each reaching movement, we compute the average of each quantity over the trials to obtain the refined measurements in Figure 1. For each reaching movement, we also show the monkey's average hand trajectory for visualization. In Figure 1, for each reaching movement, we show the average firing rate, for which the computation is explained in subsection 1.1, instead of the average spike train.

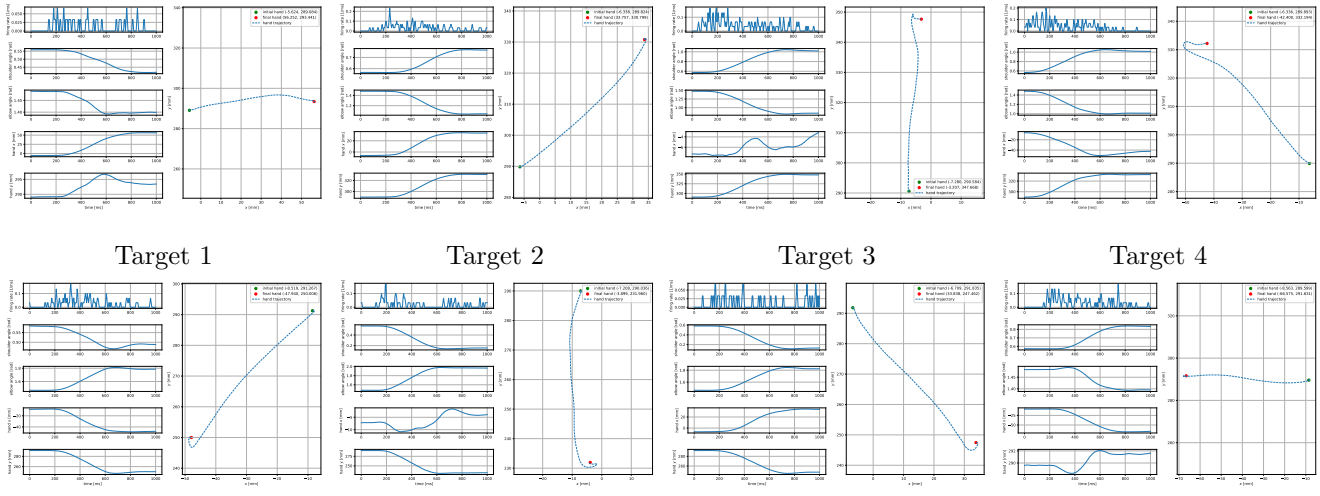

Target 1 Target 2 Target 3 Target 4

Target 5 Target 6 Target 7 Target 8

Figure 1: Data for the 8 Average Planar Reaching Movements of the Monkey's Hand

In Figure 2, we show the 8 average monkey's hand trajectories and we see that the 8 targets form approximately a circle and the 8 average initial positions of the monkey's hand are nearly the same, for each reaching movement we begin approximately at the center of the approximate circle formed by the 8 targets. For information, we suppose that the monkey always reaches the target and as we don't have access to the positions of the targets, we use the average final monkey's hand positions as approximations of the target positions.

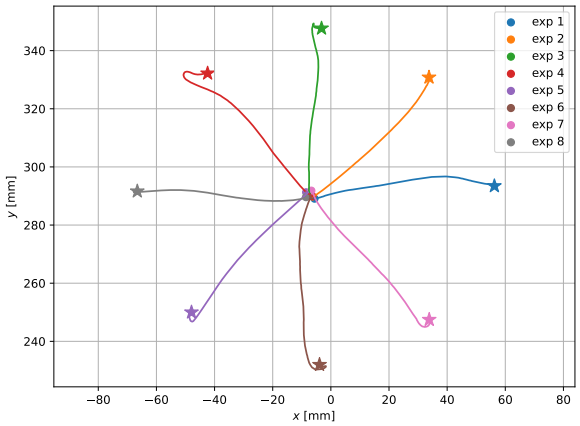


Figure 2: Visualization of the 8 Average Monkey's Hand Trajectories

## 1.1 Firing Rate

The firing rate $\rho(t)$ is defined as the convolution of the spike train $S(t)$ with a kernel function $\kappa(t)$, see (1).

$$\rho(t) := \kappa(t) * S(t) = \int \kappa(s)S(t-s)ds \tag{1}$$

We choose the rectangular kernel $\kappa(t) = (\Delta t)^{-1}\mathbf{1}_{\{0\leq t\leq \Delta t\}}$. With this kernel, the firing rate $\rho(t)$ has an intuitive meaning: the spike count in sliding interval of size $\Delta t$, $\rho(t) = \frac{n(t,t+\Delta t)}{\Delta t}$. For the data, as the time levels are sampled at 200 [Hz], there are 199 subintervals in an interval of 1 [s], so $\Delta t = \frac{1000}{199}$ [ms]. We choose the same $\Delta t$ for the kernel by simplicity.

## 1.2 Cell's Preferred Direction

The fact that the 8 targets form approximately a circle means that we have the neural data for all the directions. Hence, the target of the reaching movement for which the average spike count is the highest gives us the cell's preferred direction. To compute the average spike count of a reaching movement we take the average of the nonzero elements in the "cells" vector over the 6 trials. We don't just count the number of "1" in the vector because some spikes have as value "2". For example, for the first reaching movement, the spike trains for the 6 trials are shown in Figure 3 and the average spike count is: $\frac{2+5+3+3+10+11}{6} \approx 5,667$.

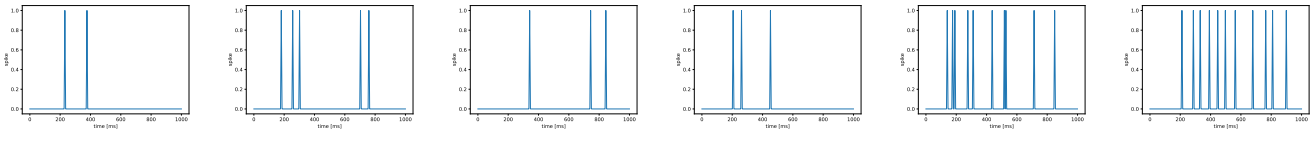

Trial 1: 2 spikes | Trial 2: 5 spikes | Trial 3: 3 spikes | Trial 4: 3 spikes | Trial 5: 10 spikes | Trial 6: 11 spikes

Figure 3: Spike Trains for the 6 Trials of the First Reaching Movement

In Figure 4, we show the cell's preferred direction in green by comparing the average spike counts of the 8 reaching movements towards the 8 different targets for which the values are given in Table 2. We observe that the direction that evokes the highest activity is the one of target 3, at position $(\sim -3.207, \sim 347.668)$, for which the average spike count is $\sim 18.1667$. We use as origin for the green vector the average initial position of the monkey's hand over the targets, it is the center of the approximate circle.

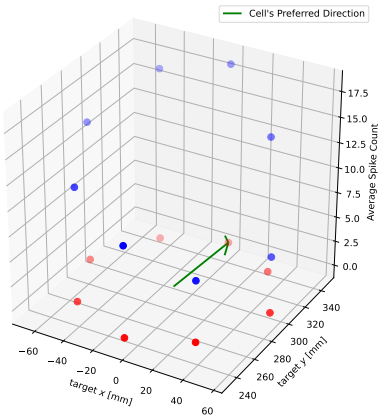


Figure 4: Cell's Preferred Direction

| Target | 1 | 2 | 3 | 4 | 5 | 6 | 7 | 8 |
|---|---|---|---|---|---|---|---|---|
| Average Spike Count | 5.667 | 13.667 | 18.1667 | 17.333 | 11.5 | 9.1667 | 6.1667 | 14 |

Table 2: Average Spike Counts for the 8 Targets

# 2 Muscle Data

To begin with, we observe that even when there is no perturbation, we do not have a perfectly straight trajectory (Type 1) 5. Regarding the perturbations, we recall that the force applied to the arm is equal to $\pm 13$ times the velocity of the hand along the y-axis. For Type 2 5, the hand is perturbed to the left because the force applied to the hand is negative. For Type 3 5, the hand is perturbed to the right because the force is positive.

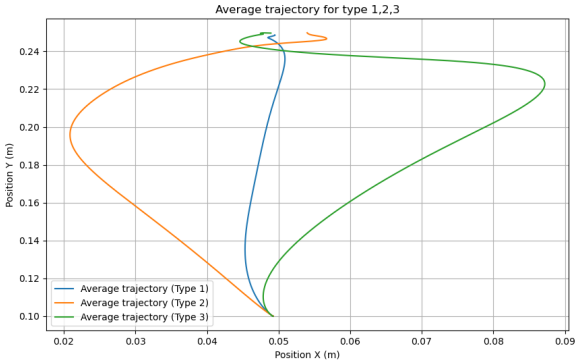


Figure 5: Average trajectory for trials type 1,2,3

## 2.1 Relationship between EMG activity and force

We noticed that the HandYForce is not directly related to the large variations in EMG activity of the deltoid and pectoralis. We will therefore focus on the relationship between HandXForce and EMG activity.

In Figure 6a, we observe that when the perturbation is to the left, it is the deltoid that activates first to counter this perturbation. The deltoid is therefore largely responsible for producing the peak in HandXForce to bring the hand back toward the target, i.e., to the right. A short time later, we also see the activation of the pectoralis, but this occurs more in a role of stabilizing the trajectory.

This observation can be explained by the biomechanics of the human body. Indeed, during a movement, muscles are divided into agonists (those that produce the movement) and antagonists (those that stabilize or oppose to prevent excessive movement). The deltoid is the primary agonist for movement to the right, while the pectoralis acts as a stabilizing antagonist to ensure balance around the shoulder joint.
Figure 6a also shows that the central nervous system uses sensory feedback loops to adjust muscle activations. For example, muscle and joint sensors detect the position and velocity of the arm. These sensory inputs allow the brain to adjust muscle activation in real time. When the sensors detect that the amplitude of the force is high, we observe that the pectoralis activates to stabilize, and the activation of the deltoid is reduced to prevent the arm from moving too far. This process helps reduce and stabilize the HandXForce around 2N. Indeed, the muscles must still generate active force to counterbalance the perturbation and maintain the arm's position.

For type 3 trials 6b, we observe that the pectoralis activates first, followed by the deltoid. This happens because the nervous system detects that the amplitude of the HandXForce becomes large toward the left. However, the deltoid ensures that the arm does not move too far to the left. This is why the HandXForce becomes positive again after the deltoid's activation. As with type 2 trials, the HandXForce tends toward 2N.

Finally, when the arm does not undergo any perturbation 6c, the force does not tend toward 2N but rather stabilizes around 1.2N, and the EMG activity is lower compared to when there is a perturbation at the end of the movement (when the velocity along the y-axis equals zero).

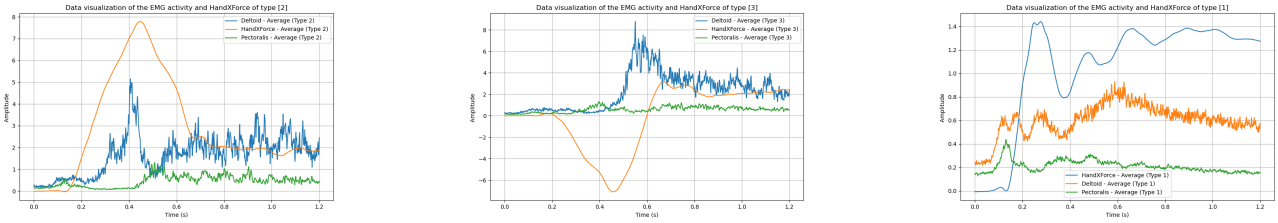


(a) Type 2 (b) Type 3 (c) Type 1

Figure 6: Comparison of EMG activity of the deltoid, pectoralis, and HandXForce across trial types.

## 2.2 Relationship between EMG activity and velocity

For the HandYVel, we observe that the velocity peak occurs after the muscle contractions at the beginning of the movement, and the perturbation has no impact on the velocity along the y-axis. Indeed, we see the same velocity curve for type 2 and type 3 trials as for type 1 trials.

For the HandXVel in type 2 trials, we see in Figure 7b that the velocity is initially negative because the perturbing force pushes the arm to the left. Then, the deltoid activates and manages to push the arm to the right, resulting in a positive velocity. The velocity tends toward zero when the participant finds the balance to counteract the perturbing force.

For type 3 trials, I can apply the same reasoning. However, we observe in Figure 7a that it is the pectoralis that generates a force to make the velocity negative, bringing the arm back to the left. Subsequently, the deltoid plays a role in stabilizing the movement and achieving a zero velocity.


(a) Type 3 (b) Type 2

Figure 7: Comparison of EMG activity of the deltoid, pectoralis, and HandXVel across trial types.

### 2.3 Anticipation of the perturbation after several trials

In addition to comparing EMG activity with hand kinematics, we also wondered whether the participant adapted as the trials progressed.

We observe in Figure 9 that the deltoid is activated earlier in trial 30 compared to trial 1. As a result, the force is generated earlier, which helps the arm limit the effect of the perturbation. Indeed, in Figure 8a, we see that the position is less perturbed in trial 30 than in trial 1.

These observations are the result of learning. At the beginning of the trials, the brain does not anticipate the perturbation, and the response time is longer. After several trials of the same type, the brain learns to anticipate the perturbation through motor memory.

Furthermore, with repetition, the time needed to produce muscle activation decreases due to the optimization of neural circuits. Repetition also allows the brain to develop a predictive internal model. This model enables the brain to anticipate the effect of the perturbation and adapt the motor command to maintain a straighter trajectory.

Thanks to this model, the motor system no longer relies solely on sensory feedback to correct errors. The existence of this model also explains why, in Figure 8b, during trial 30, the hand moves directly toward the target without veering too far to the left. The same stability can be observed in Figure 8a.

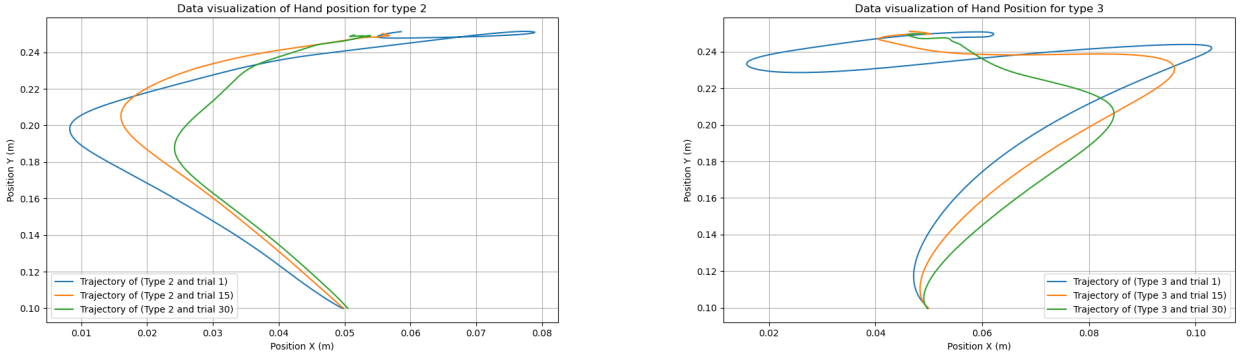


(a) Type 2

(b) Type 3

Figure 8: Position with adaptation for type 2 and 3

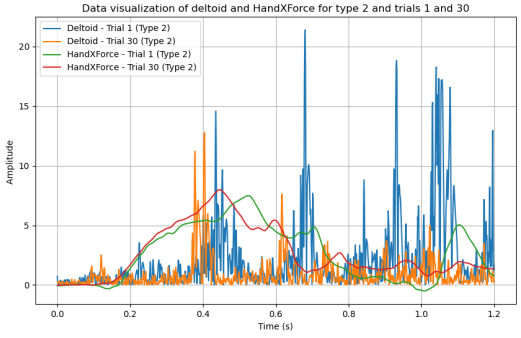


Figure 9: EMG deltoid and HandXForce for type 2

## 3 Bonus

We already have the average monkey's hand trajectories towards the 8 targets.
We use the average initial monkey's hand positions as the initial conditions and the average final monkey's hand positions as the 8 targets to simulate the 8 planar reaching movements towards the 8 different targets with the SOC

implemented for the Project 1. We choose a simulation time of 1 [s] and we sample the time levels at 200 [Hz] as the preprocessed data for this Project are measured over a timespan of 1[s] and sampled at 200 [Hz]. We must be careful with the units because in Project 1 we used [m] and [s] while in this Project we use [mm] and [ms].

The steps to obtain the 8 SOC's hand trajectories towards the 8 targets:

1. In the code of Project 2, we compute the vectors with the average initial and final monkey's hand positions. The latter are in [mm], we must convert them to [m] to use them in the code of Project 1.
2. We copy and paste those vectors in the code of Project 1.
3. For each pair of average initial and final monkey's hand positions, we simulate the trajectory of the SOC by solving the system dynamics with the code of Project 1.
4. We obtain the SOC's hand trajectories for the 8 reaching movements in [m]. We must convert them to [mm] to use them in the code of Project 2.
5. We copy and paste the vectors with the SOC's hand trajectories in the code of Project 2.
6. We plot the hand trajectories of the monkey and the SOC towards the 8 targets for comparison. Do they look alike ? Who is better ?

Our generic object oriented code of the Project 1 makes it easy to perform those simulations. The extra work done for Project 1 is now paying off in this Project. The comparison between the performance of the monkey and the SOC is shown in Figure 10. We observe that the trajectories look alike, which means that our simulations with the SOC reproduce real-life hand trajectories, which is good. Moreover, except for the reaching movement towards target 8, the one at the left, the hand trajectories of the SOC are better than the ones of the monkey because they are shorter. This means that the work done by the SOC is in general smaller than the one done by the monkey, so the SOC consumes less energy. This is thanks to the following terms in the minimized cost function $J(\mathbf{x}, \mathbf{u})$ representing the energetic cost: $u_k^T R u_k$, $k \in \{1, ..., N-1\}$. Our SOC performs better than the monkey thanks to Mathematics :)

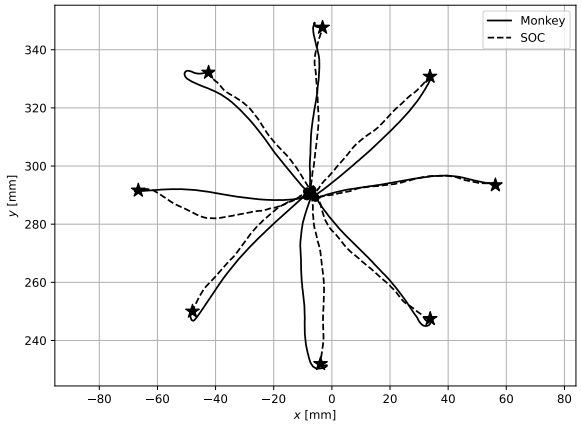


Figure 10: Comparison between the Hand Trajectories of the Monkey and the SOC